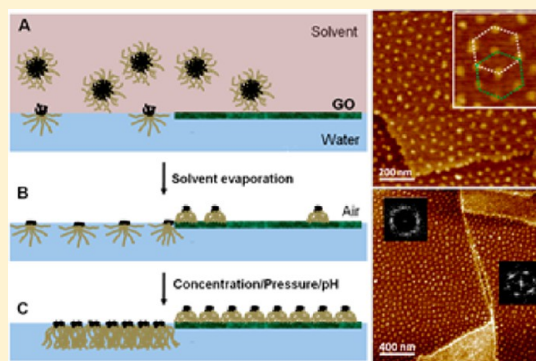


Star Polymer Unimicelles on Graphene Oxide Flakes

Ikjun Choi,[†] Dhaval D. Kulkarni,[†] Weinan Xu,[†] Constantinos Tsitsilianis,[‡] and Vladimir V. Tsukruk^{*,†}[†]School of Materials Science and Engineering, Georgia Institute of Technology, Atlanta, Georgia 30332-0245, United States[‡]Department of Chemical Engineering, University of Patras, 26504 Patras, Greece, and Institute of Chemical Engineering and Sciences (FORTH/ICE-HT), Greece

S Supporting Information

ABSTRACT: We report the interfacial assembly of amphiphilic heteroarm star copolymers ($\text{PS}_n\text{P2VP}_n$ and $\text{PS}_n(\text{P2VP-}b\text{-PtBA})_n$ ($n = 28$ arms)) on graphene oxide flakes at the air–water interface. Adsorption, spreading, and ordering of star polymer micelles on the surface of the basal plane and edge of monolayer graphene oxide sheets were investigated on a Langmuir trough. This interface-mediated assembly resulted in micelle-decorated graphene oxide sheets with uniform spacing and organized morphology. We found that the surface activity of solvated graphene oxide sheets enables star polymer surfactants to subsequently adsorb on the presuspended graphene oxide sheets, thereby producing a bilayer complex. The positively charged heterocyclic pyridine-containing star polymers exhibited strong affinity onto the basal plane and edge of graphene oxide, leading to a well-organized and long-range ordered discrete micelle assembly. The preferred binding can be related to the increased conformational entropy due to the reduction of interarm repulsion. The extent of coverage was tuned by controlling assembly parameters such as concentration and solvent polarity. The polymer micelles on the basal plane remained incompressible under lateral compression in contrast to ones on the water surface due to strongly repulsive confined arms on the polar surface of graphene oxide and a preventive barrier in the form of the sheet edges. The densely packed biphasic tile-like morphology was evident, suggesting the high interfacial stability and mechanically stiff nature of graphene oxide sheets decorated with star polymer micelles. This noncovalent assembly represents a facile route for the control and fabrication of graphene oxide-inclusive ultrathin hybrid films applicable for layered nanocomposites.



■ INTRODUCTION

Graphene oxide (GO), which is derived from an oxygenated graphene lattice, is an emerging two-dimensional material with its intriguing electronic, electrochemical, and biological activity.^{1–3} Modification of graphene oxide chemistry with metal nanoparticles,^{4,5} DNA aptamers,⁶ peptides,^{7,8} and polymers^{9,10} through covalent/noncovalent interactions (e.g., various chemical groups such as hydroxyl, amine, charged glutamic acid, and aromatic amino acid) is an area of current research interest in electrochemical and biosensing devices with enhanced sensitivity and selectivity. Graphene oxide, as a graphene precursor, can be dispersed in water and thus enables wet chemistry and solution processes for a variety of thin film fabrication. The monolayer graphene oxide flake is considered a single atom layer carbon material with a wide range of sizes and shapes, which comprises hydrophobic graphitic domains (irregular regions of 1–6 nm² across) randomly distributed in hydrophilic oxygenated regions with the overall average ratio of graphitic:oxygenated:vacancy areas of 16:82:2%, which is concerted with the popular Lerf–Kilnowshik (LK) model.^{11,12}

The exact source of high acidity of graphene oxide and localization of acidic groups still remains arguable.¹³ The presence of polar bondings including hydroxyl, phenol, epoxide, and carboxylic acid groups on the edge and basal plane is an

evident cause of compelling solubility of graphene oxide flakes, enabling diverse chemical interactions such as electrostatic, van der Waals, hydrogen bonding, and π – π interactions available for interfacial assemblies.¹⁴ Control over interactions and assemblies between graphene oxide and functional components is crucial because it affects complexation behavior, interfacial structure, and overall integrity, morphology, and ultimate nanocomposite performance.^{15,16}

The geometrically anisotropic (i.e., large aspect ratio in lateral and vertical direction) and unique in-plane random heterogeneous character due to the distribution of hydrophobic and hydrophilic domains is known to be critical for the stabilization of graphene oxide sheets at the fluid–fluid interface (e.g., air–water and solvent–water).² Specifically, in recent work, Huang and his colleagues have demonstrated a facile and versatile approach to control assembly of monolayer graphene oxide (i.e., up to micrometer scale uniformity) on the Langmuir trough. The in-plane amphiphilic feature combined with the use of a methanol/water (5:1) mixed solvent system allowed graphene oxide to spread on the water surface and

Received: April 26, 2013

Revised: July 1, 2013

Published: July 7, 2013

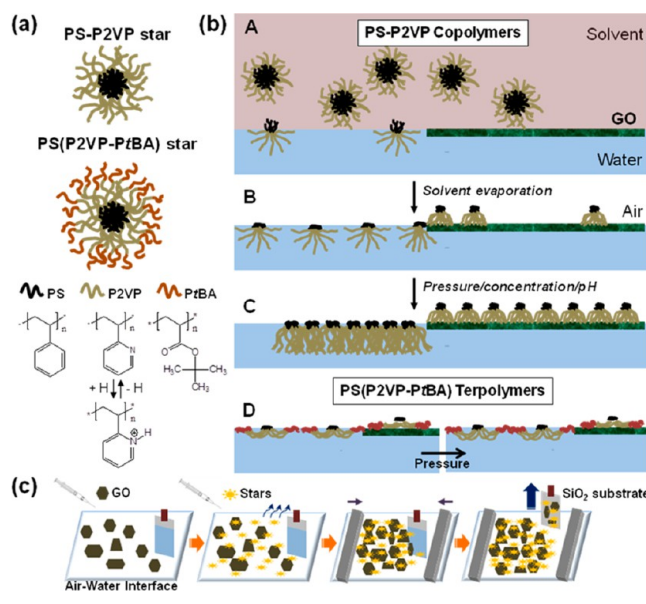
subsequently remain afloat via “edge-to-edge” repulsion after evaporation of methanol, which experimentally validated its amphiphilic nature.^{17,18} While hydrated pliable graphene oxide in solution and bulk has a corrugated configuration due to the presence of vacancy and compositional inhomogeneity, it is able to transform into a stretched flat structure driven by capillary force and surface tension when incorporated at the interface.¹⁹ For example, assembly of graphene oxide as a two-dimensional filler for polymer nanocomposites has been explored for the fabrication of ultrathin nanomembranes in our research group. Surface-assisted assembly approach via electrostatic and hydrogen-bonding interactions between graphene oxide and synthetic polyelectrolyte or silk fibroin led to highly integrated hierarchical multilayer films with minimized folding and wrinkling showing dramatically enhanced mechanical properties of flexible nanocomposites with low graphene oxide content (8–20 vol %).^{20,21}

Surface-active properties of graphene oxide have been further manifested in the graphene oxide-assisted emulsification of toluene in aqueous media, and the interfacial entrapment of graphene oxide induced by air bubbles in aqueous solution.²² At the fluid–fluid interface (i.e., nonaromatic polar solvent chloroform/water interface), in particular, the organic solvent-driven enrichment of graphene oxide sheets from the bulk solution is another example to support their surface activity.²³ These findings are indeed extending the ability of graphene oxide flakes for assembly and functionalization, which are important for the fabrication of organized nanocomposites. In this regard, interfacially driven assembly through noncovalent interactions can be considered for large area fabrication of flexible organized nanocomposite materials with anisotropic structure, controlled adsorption, and minimized wrinkling and folding.

Recently, noncovalent attachments based on self-assembly of amphiphilic star polymers have been considered for stabilizing carbon-based materials in solution.²⁴ Iatridi et al. demonstrated that polystyrene/(poly(2-vinylpyridine)-*b*-poly(acrylic acid)) star terpolymer (PS₂₂(P2VP-*b*-PAA)₂₂) enabled the pH tunable stabilization of carbon nanotubes in aqueous media, leading to a controlled dispersion of colloidal nanotube-star hybrid via noncovalent bonding interactions.²⁵ Gröschel et al. proved the concept that polymer-based Janus micelles can be utilized as effective colloidal dispersants in a variety of solvents.²⁶ However, no attempts to assemble star polymers with heterogeneous chemical composition on graphene oxide sheets have been reported to date.

Here, we report the assembly of graphene oxide sheets with surface-active macromolecular surfactant, amphiphilic star copolymer, at the air–water surface (Scheme 1). The highly branched poly(styrene)-poly(2-vinylpyridine) (PS-P2VP)_n star copolymers comprising hydrophobic (PS) and hydrophilic arms (P2VP with ionizable pyridine groups)²⁷ were chosen to pair with heterogeneous graphene oxide sheets. The binding, spreading, and assembly behavior of the star copolymers in the form of unimicelles at the edge and on the basal plane of graphene oxide flakes was investigated using the Langmuir–Blodgett (LB) technique for different polymer/graphene oxide mixing ratios, surface pressure, and spreading solvent polarity. This surface-mediated assembly led to stable micelle–graphene oxide bilayers. Incompressible and highly ordered micelle morphology on the graphene oxide surface is caused by strong affinity between two components and stable polymer–graphene oxide complexes.

Scheme 1. (a) Chemical Structure of Amphiphilic Heteroarm PS₂₈P2VP₂₈ Star Copolymer and PS₂₈(P2VP-*b*-PtBA)₂₈ Star Terpolymer; (b) Assembly and Suggested Molecular Conformation of Star Polymer Surface Unimicelles on Graphene Oxide Sheets at Solvent/Water and Air/Water Interfaces for Star Copolymers (A–C) and Star Terpolymers (D); and (c) Fabrication Process of GO/Star Polymer Composite Monolayer at Air–Water Interface on LB Trough: (1) GO Spreading; (2) Star Copolymer Spreading Followed by Solvent Evaporation; (3) Applying Lateral Compression; and (4) Pulling Off Silicon Substrate across Air–Water Interface from Water Subphase in a Vertical Direction for Transferring to Silicon Substrate



EXPERIMENTAL SECTION

Materials. Graphene oxide was prepared from natural graphite flakes (325 mesh, 99.8% metal basis) purchased from Alfa Aesar through Hummer’s method.¹ The dispersion of graphene oxide in a solution mixture of methanol/water (5:1 volume ratio) was subjected to ultrasonication for 15 min followed by centrifugation at 3000 rpm for 45 min. The supernatant (concentration 0.01 wt %) was decanted and used for all experiments. The average surface roughness is 0.15 ± 0.05 nm (over a $500 \text{ nm} \times 500 \text{ nm}$ surface area), indicating an atomically smooth monolayer that is consistent with a previous study.²⁰

Star Block Copolymers. The “in–out” methodology for star polymer synthesis was followed for the preparation of PS₂₈(P2VP-*b*-PtBA)₂₈ heteroarm star block terpolymer and its PS₂₈P2VP₂₈ copolymer precursor as reported elsewhere.²⁸ Briefly, the star terpolymer was prepared by “living” anionic polymerization in a one-pot/four-step reaction. In the first step, the PS arms were prepared in THF, using *s*-BuLi as the initiator. After the consumption of styrene, the “living” PS chains were used to polymerize a small quantity of DVB (cross-linking agent), resulting in a “living” star-shaped polystyrene precursor (PS_n) bearing active sites in its PDVB core. In a next step, the “living” star was used to polymerize 2VP, leading to the formation of a second generation of P2VP arms. Part of the reaction medium was sampled out for the isolation, purification, and characterization of the PS₂₈P2VP₂₈ star copolymer. Subsequently, the sites located at the end of P2VP arms were used to polymerize *t*BA. The final PS₂₈(P2VP-*b*-PtBA)₂₈ terpolymer was obtained after complete consumption of the monomer and protonation of the active sites, and thereby there are no specific end groups. The terpolymer was characterized by means of size exclusion chromatography (SEC) and static light scattering (SLS). The number of arms have been calculated from the molecular weight of the PS star precursor (by LS)

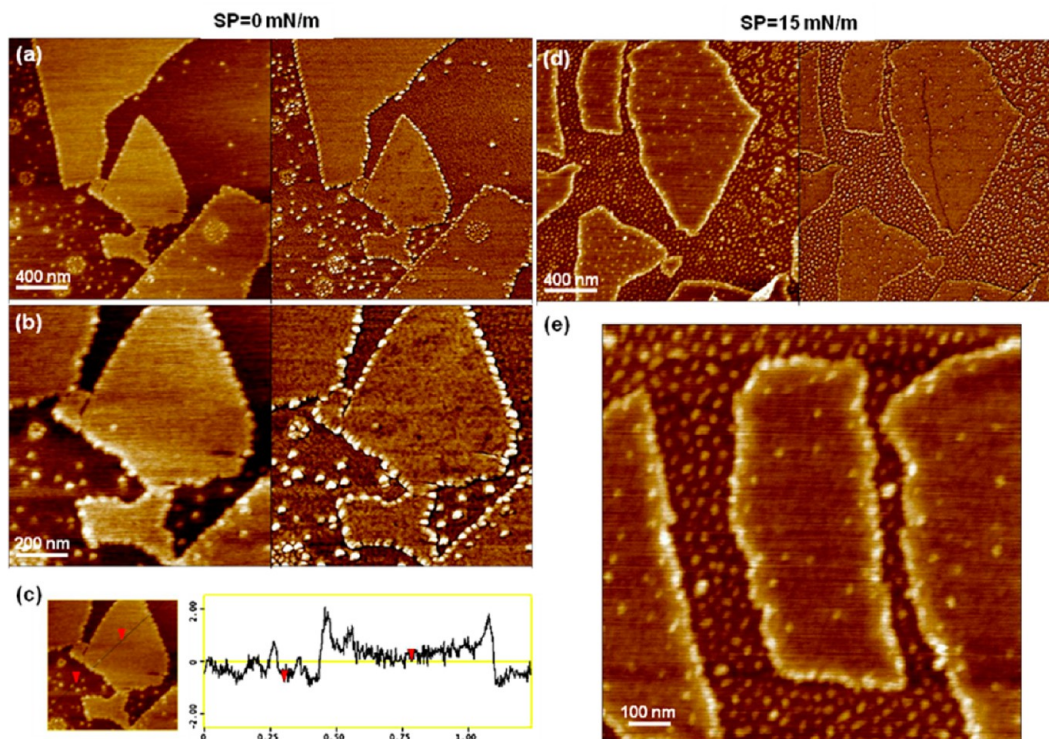


Figure 1. AFM topography (left) and phase (right) of GO (0.01 wt %, 0.5 mL)/PS₂₈P2VP₂₈ star copolymer (0.02 mg/mL in chloroform, 70 μ L): (a) large area scan, (b) high-resolution zoomed-in image, and (c) topography height profile of corresponding image from (b) at surface pressures of 0 mN/m (a–c); (d) large area scan and (e) high-resolution zoomed-in for surface pressure 15 mN/m (d,e). The subphase pH was adjusted at pH 2. z-scale: 5 nm (topography) and 30° (phase) for (a,d); 3 nm (topography) and 20° (phase) for (b,c,e).

subtracting the poly(divinyl benzene) core and then dividing by the molecular weight of the PS arms (by GPC). The corresponding results are presented in Table S1 (see the Supporting Information).^{27,28}

Substrate Preparation. Freshly cut silicon substrates with dimensions 1 cm \times 2 cm and [100] orientation (University Wafer) and a native silicon dioxide layer having a 1.6 nm thickness were cleaned with piranha solution (3:1 concentrated sulfuric acid and hydrogen peroxide mixture, hazardous mixture) in accordance with the usual procedure.²⁹ Subsequently, they were abundantly rinsed with Nanopure water (resistance >18.2 M Ω cm, Barnstead) and dried with a dry nitrogen stream. Pretreated substrates served as a hydrophilic planar substrate for film deposition.

Fabrication of Graphene Oxide/Star Polymer Structures. Interfacial assembly of graphene oxide sheets and star polymers at the air–water interface was conducted on a KSV2000 mini trough equipped with a Wilhelmy plate for pressure sensing according to the usual procedure.³⁰ All experiments were made at a constant temperature of 25 $^{\circ}$ C in a clean environment. Nanopure water was used as the subphase for all experiments. The pH of the water subphase was adjusted by using hydrochloric acid and sodium hydroxide without a buffer system.

The graphene oxide sheets were spread first at the air–water interface followed by depositing star polymer solution (Scheme 1c).⁴⁸ Solutions of 0.2–0.1 mg/mL of a star copolymer were dissolved in various solvents including chloroform, tetrahydrofuran, toluene, and dichloromethane (HPLC grade), and 70 μ L of the polymer solution was spread uniformly at the air–water interface and was allowed to evaporate for 30 min prior to compression. The compression of Langmuir monolayers was conducted at a speed of 5 mm/min, and then monolayers were transferred onto a silicon wafer by a vertical dipping method at a dipping rate of 2 mm/min and different surface pressures (0, 15, and 30 mN/m).

Surface Morphology Characterization. The morphology of graphene oxide/star polymer structures was probed under ambient conditions in air using a Dimension 3000 atomic force microscope

(AFM) (Veeco Inc.). For quantitative analysis of surface topography, AFM images were obtained in the “light” tapping mode with an amplitude ratio within 0.90–1.00 to avoid surface damage and deformation.³¹ The AFM cantilevers had spring constants in the range of 40–60 N/m. Scanning rates were between 1.0 and 2.0 Hz, depending on the scan area, which ranged from 10 μ m \times 10 μ m to 1 μ m \times 1 μ m. Electrostatic force images were obtained with a Bruker Icon AFM using a p-doped silicon cantilever with a spring constant of 3 N/m and resonant frequency of 65 kHz. Adhesion, modulus, and deformation maps were obtained using the Quantitative Nano-mechanical Measurements (QNM) mode on the Bruker Icon AFM.³² The Raman mapping was performed with a WITec (Alpha 300R) confocal Raman microscope using an Ar ion laser (λ = 514.5 nm) as an excitation source according to the usual procedure. The spectrum was obtained using a 600 grooves mm⁻¹ grating with a spectral resolution of 5 cm⁻¹. All of the measurements were conducted for LB monolayers in the dry state on the silicon oxide substrates under the common assumption that the monolayer morphology is not affected significantly by its transfer from the air–water interface.

RESULTS AND DISCUSSION

Effect of Concentration and Surface Pressure.

According to previous reports, the amphiphilic PS₂₈P2VP₂₈ star copolymer used in this study has been known to show pH-dependent surface aggregation behavior and a stable Langmuir monolayer composed of unimolecular micelles (or unimicelles) at the air–water interface.^{33–38} The pressure–area (π – A) Langmuir isotherm of GO/PS₂₈P2VP₂₈ star copolymer showed gradual compression up to 40 mN/m, which is higher than individual graphene oxide and star copolymer, indicating the formation of a stable surface assembly at the air–water interface (Figure S1). The surface morphology images of the star polymer/graphene oxide LB films were all acquired from silicon oxide substrates in the dry state.

To investigate the binding behavior of star copolymer unimicelles, a lower concentration of star copolymer solution (0.02 mg/mL PS₂₈P2VP₂₈ star copolymer in chloroform) was spread without external compression ("apparent" surface pressure = 0 mN/m). Acidic pH conditions were chosen (pH = 2), which allowed the pyridine units of P2VP segment to protonate and impart a positive charge on the arms (degree of ionization up to 60%, $pK_{a,P2VP} \approx 5.2$).³³ The zeta-potential of graphene oxide at pH = 2 falls in the range of -10 to -20 mV.¹⁴ Thus, sufficient Columbic repulsion can be achieved to stabilize the graphene oxide monolayer film at the air–water interface.

At zero pressure, deposition of star copolymers resulted in decoration of the polygonal periphery of graphene oxide sheets with star copolymer unimicelles, while a small number of star polymer unimicelles were found on the basal plane (Figure 1). High-resolution AFM image shows that the spherical micelles bonded predominantly along the edges of graphene oxide sheet with sparse concentration on the basal plane, especially on top of the edge (total graphene oxide/micelle thickness: 2.0 ± 0.3 nm) (Figure 1b,c). Moreover, single micelle-string features were observed without aggregation along the edges of the graphene oxide. This interesting morphology suggests that star copolymer unimicelles tend to move closer to the edge of graphene oxide sheets upon evaporation of star copolymer solution. Solution spreading/evaporation might trigger accumulation at the edge in combination with the relatively hydrophobic graphene oxide basal plane as compared to the water surface. Also, graphene oxide under acidic conditions (pH ≈ 2) is known to show a higher contact angle ($\sim 70^\circ$) with water than the graphene oxide at higher pH (60° for basic water of pH 10). This suggests a reduced wettability of graphene oxide by water under the conditions employed in our study.³⁹

Upon compression to a surface pressure of 15 mN/m, the surface density of star copolymer unimicelles formed at the air–water interface increased significantly, while the density at the surface of graphene oxide sheets still remained very low (Figure 1d,e). It is worth noting that the AFM images shown in Figure 1 and the following figures were obtained by transferring the LB monolayer on a solid silicon oxide substrate, but represent different scenarios at the original fluid interface: polymer monolayer is formed on either graphene oxide sheets or directly at fluid surface (Scheme 1). The density of star polymer unimicelles at the graphene oxide edge remains similar upon compression, as is evident from the high-resolution AFM topography image in Figure 1e. Also, comparing Figure 1a and d, no significant difference in micelle density was observed on the basal plane of the graphene oxide sheets.

For further comparison of the effect of star copolymer concentration on preferential binding and assembly on the graphene oxide surface, a high concentration of the star copolymer solution was deposited (0.1 mg/mL of PS₂₈P2VP₂₈ star copolymer in chloroform) at the same subphase pH of 2. These conditions resulted in a uniform surface coverage with compact organization across both graphene oxide and water surfaces. A local 6-fold symmetry of star copolymer domain packing on the graphene oxide sheets was observed, indicating a uniform behavior under compression, and corresponds to the dense surface packing of symmetrical disc-like molecules with a central core height of 1.3 ± 0.3 nm (Figures 2 and 3). The protonated stretched P2VP arms are expected to dominate the spacing and ordering of spherical polymer micelles due to

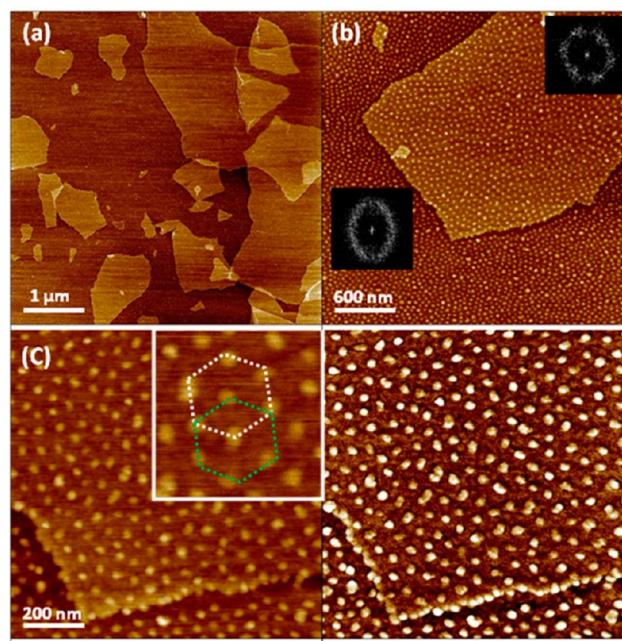


Figure 2. AFM topography (left, a–c) and phase (right, c) of GO (0.01 wt %, 0.5 mL)/PS₂₈P2VP₂₈ star copolymer (0.1 mg/mL in chloroform, 70 μ L) at pH 2 for surface pressures of 0 mN/m. The inset in (c) indicates lattice analysis from the corresponding topography image in (c). z-scale: 5 nm (topography) and 20° (phase).

intra-/intermolecular electrostatic and entropic repulsion. It has been demonstrated previously that the star copolymer unimicelles having a core–shell structure induced by phase segregation at pH 2 with the collapsed PS core on top of the extended P2VP shell (single PS₇P2VP₇ copolymer with P2VP molecular weight ($M_{w,P2VP arm}$) of 56 500 Da) had an average diameter of 126 nm (highly stretched state) and 2.9 nm domain height.^{41,48} On the basis of these results and the assumption that the chain dimensions are directly proportional to the molecular weight, we can estimate that the diameter of PS₂₈P2VP₂₈ star copolymer ($M_{w,P2VP arm} = 16\ 000$ Da) used in this study is around 36 nm. Taking into account the higher number of arms (28 versus 7 arms), this value can be increased presumably due to increased intramolecular repulsion.

As is apparent from Figure 2b and c, spacing between the spherical surface micelles was larger (69 ± 12 nm) on graphene oxide surface than on the water surface (43 ± 8 nm), indicating a packed state of star macromolecules suited on the fluidic subphase (about 2 times smaller cross-sectional surface area per molecule). In the previous study, we have observed that the dimension of PS₂₈P2VP₂₈ star copolymer from LB monolayer was 64 ± 5 nm in diameter with an effective thickness of 0.5 nm.³⁸ Thus, the star polymer on the graphene oxide sheets seems to have a similar stretched conformation; however, a decrease in size of star polymers was observed at the water surface. On the other hand, the predeposition of graphene oxide sheets at the air–water interface results in a reduced free surface and thereby more densely packed state of the star polymers at the same concentration. As illustrated in Scheme 1b (A–C), amphiphilic star copolymers can be predicted to undergo different extents of conformational transition on graphene oxide sheets and water surface (from initial planar surface micelle into compressed and compact structure with vertical orientation under external environments).⁴⁰ Also, the AFM imaging directly visualized the interface line along which

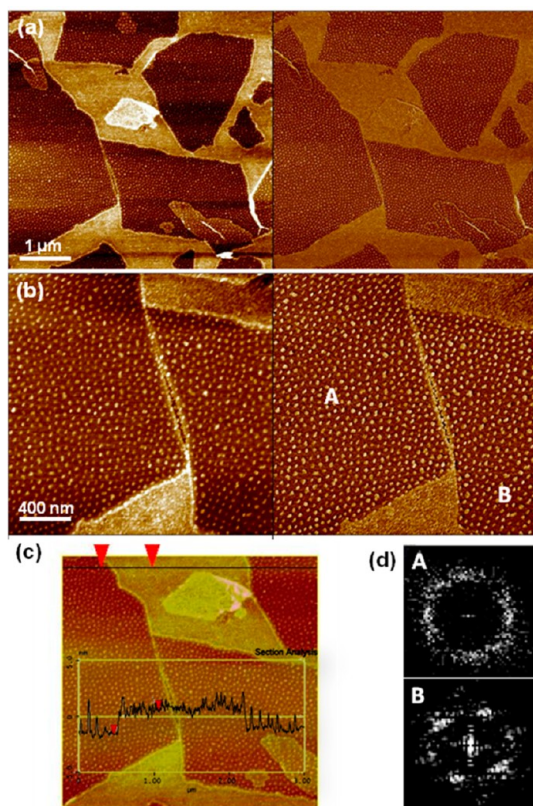


Figure 3. AFM topography (left) and phase (right) of (a,b) GO (0.01 wt %, 0.5 mL)/PS₂₈P2VP₂₈ star copolymer (0.1 mg/mL in chloroform, 70 μ L) at pH 2 for surface pressures of 15 mN/m; (c) the height profile of the corresponding topography image; and (d) FFT of domain morphologies for A and B regions from (b) where A is corresponding to the center region while B represents the near edge region of GO sheet. z-scale: 5 nm (topography) and 30° (phase).

the edge of graphene oxide sheet meets the continuously organized star copolymer monolayer (0 mN/m) at the air–water interface (Figure 2).

The sharp interface between graphene oxide sheets and highly compressed star copolymer monolayer was more pronounced at higher pressure (15 mN/m) (Figure 3). Polymer micelles appear to be ordered along the graphene oxide edge, while more symmetrical hexagonal packing was prominent on the basal plane farther from the edges (Figures 2b,c and 3b,d). We note that the average domain spacing (66 ± 13 nm) on the graphene oxide remained almost unchanged during compression. However, the packing of the star polymers was very dense on the water surface. This observation revealed that the star polymer micelles stay incompressible on the surface of graphene oxide sheets under compression with reduced surface area of polymer monolayer between sheets.

Also, it is interesting that the polymer monolayer thickness difference on the basal plane of graphene oxide sheets and at the water surface is more pronounced upon compression. The AFM sectional analysis revealed that the top surface of compressed polymer monolayer on the water surface is around 1.5 nm thicker than that on the graphene oxide surface, indicating that a change in molecular conformation of the star copolymers occurs as a response to external compression with arms extending into the water subphase (Figure 3c). Further, a clearly distinguished interface between the graphene oxide sheets and densely packed polymer monolayer indicates that

there is no occurrence of buckling or folding of the polymer monolayer along the edges of graphene oxide sheets under high compression. This result also suggests that the edges of graphene oxide sheets locate at the air–water interface rather than sink into the subphase during compression (Scheme 1).

To further investigate the characteristics of the edge/basal plane of the graphene oxide sheets and the polymer monolayer, high-resolution QNM measurements were carried out over a selected area under the same conditions (Figures 4 and S2).

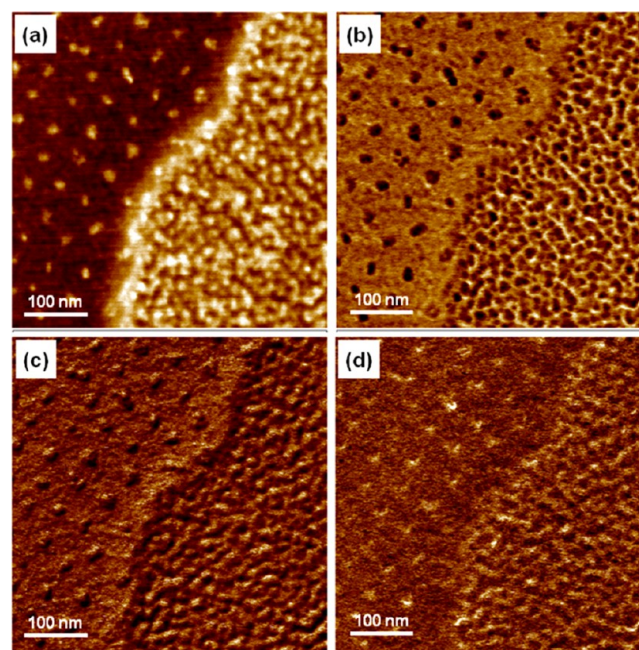


Figure 4. High-resolution QNM analysis of (a) topography, (b) adhesion, (c) apparent modulus, and (d) deformation for GO (0.01 wt %, 0.5 mL)/PS₂₈P2VP₂₈ star copolymer (0.1 mg/mL in chloroform, 70 μ L) at pH 2 for surface pressures of 15 mN/m. z-scale: 4 nm (topography), 2.5 nN (adhesion), 1.61 GPa (modulus), and 1.3 nm (deformation).

The topographical image shows closely packed star copolymer micelles on the silicon oxide (corresponding to the air–water surface areas on the LB trough). This morphology can be attributed to the tendency of the stars to undergo a conformational transformation from pancake to brush conformation due to swelling and extension of hydrophilic pyridine segments toward the water subphase under lateral pressure.⁴⁰ It is important to note that at the borderline between the graphene oxide and water surface, star copolymer micelles appear to be highly crowded, but no obvious invasion of polymer micelles toward the graphene oxide basal plane is observed.

The adhesion images clearly differentiate the polymer micelles and graphene oxide surface, showing low adhesive forces on hydrophobic PS domains and much higher adhesion for surrounding hydrophilic polar regions of spread P2VP arms (Figure 4b). Also, the apparent modulus mapping confirms higher stiffness of central domains as compared to the stiffness of surrounding matrix of spread arms. It is worth noting that the elastic modulus cannot be measured correctly due to the high stiffness of the graphene oxide and the oxide substrate underneath.

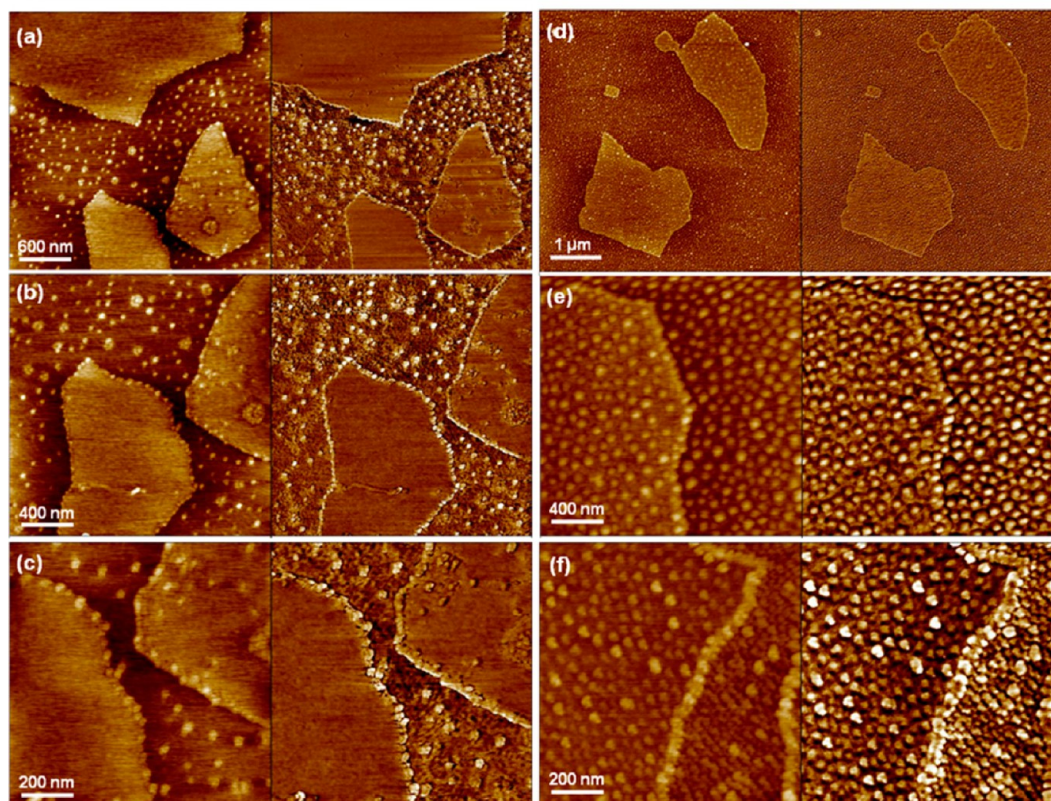


Figure 5. AFM topography (left) and phase (right) of (a–c) GO (0.01 wt %, 0.5 mL)/PS₂₈(P2VP-PtBA)₂₈ star terpolymer (0.02 mg/mL in chloroform, 70 μ L) at surface pressures of 0 mN/m, (d,e) GO (0.01 wt %, 0.5 mL)/PS₂₈(P2VP-*b*-PtBA)₂₈ star block copolymer (0.1 mg/mL in chloroform, 70 μ L) at surface pressures of 0 mN/m, (f) GO (0.01 wt %, 0.5 mL)/PS₂₈(P2VP-*b*-PtBA)₂₈ star block copolymer (0.1 mg/mL in chloroform, 70 μ L) at surface pressures of 15 mN/m. All depositions were conducted at pH 2. z-scale: 5 nm (topography) for (a–f) and 30° for (a); 20° for (b,c); and 10° for (d–f) (phase).

A further increase in the surface pressure does not change the symmetry and spacing of polymer domain morphology on the graphene oxide surface (see high-resolution images in Figures 2 and 3). However, patterned spherical micelle morphology of polymer monolayer was found to transform into interconnected lamellar or layered continuous morphology on the water surface, thus indicating dominant compression of polymer monolayer located between sheets (Figures 3 and 4). It is apparent that compressive stresses are not directly transferred to polymer monolayers on graphene oxide sheets, thus preserving “starfish” global conformation, and the polymer–graphene oxide complexes become more stable against compression.

Reduction of surface area at the air–water interface is facilitated by the transformation of the highly ionized P2VP segments at the water surface, which can easily sink into the water subphase to form brush-like conformation as was demonstrated in previous studies on similar star block copolymers.^{41–44} This is likely due to the pH-sensitivity of the P2VP blocks ($pK_{a,P2VP} \approx 5.2$), which protonate under acidic pH conditions (pH = 2) and are prone to submerge into the water subphase upon modest compression. These properties facilitate the conformational transition from “starfish” to “jellyfish” global conformation if star macromolecules are located at the water surface.^{38,45} We suggest that as a result of such heterogeneous morphology with different lateral and vertical segregation of star macromolecules, vertically segregated unimicelles cannot cross over the elevated graphene oxide sheet edges and homogenize the conformational state of star

macromolecules across the whole film. We believe that such stable surface micelles on graphene oxide sheets result from decreased configurational entropy of branched arms confined on the attractive and nondiffusive graphene oxide surface. Overall, such “engineered” biphasic morphology of Langmuir polymer monolayer represents a nontrivial example of tailored bicomponent polymer monolayers rarely observed for Langmuir monolayers.

Effect of Molecular Composition. Another intriguing feature of these biphasic monolayers was the preferential decoration of the sheet edges with individual polymer micelles of different star terpolymer, PS₂₈(P2VP-*b*-PtBA)₂₈, having a hydrophobic nonaromatic end block (PtBA) (Figure 5, Table S1). It is noteworthy that star terpolymers were prominently bound along the edge of graphene oxide at low concentrations (Figure 5a–c), while a dense coverage of star terpolymer micelles was observed everywhere at high polymer concentration with the edges still maintaining a dense chain-like morphology of the star polymers (Figure 5d–f). Also, star terpolymers retain a circular micelle on the water surface under compression. We suggest that the hydrophobic PtBA end blocks promote a pancake conformation and play an unfavorable role in brush-like conformational transformation by preventing the hydrophilic P2VP midblock from completely sinking into the water subphase in contrast to star copolymer with free P2VP end-blocks (Scheme 1b). The chain entropic effect seems to be dominant in dictating the assembly behavior as compared to end block polarity. Sterically restricted P2VP arms of the terpolymers in 2D confined conformation are

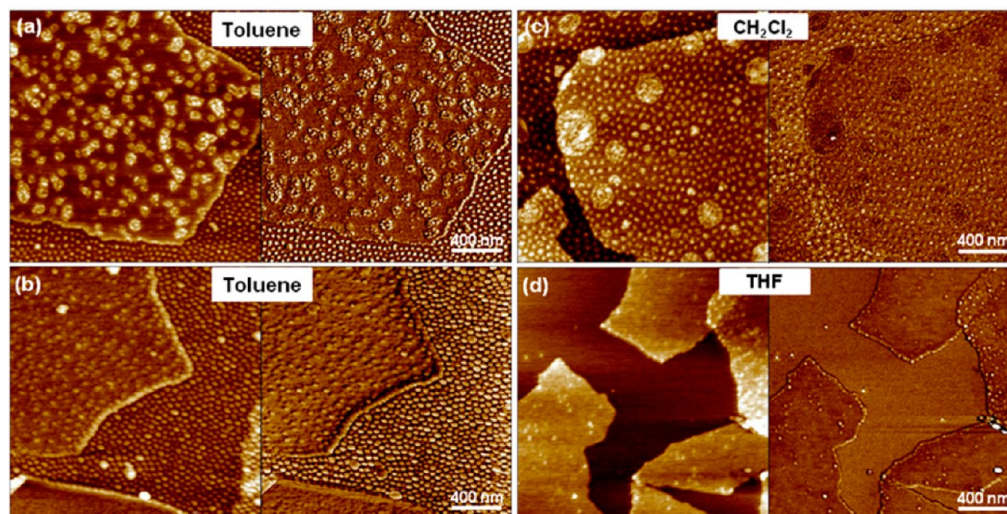


Figure 6. AFM topography (left) and phase (right) of GO (0.01 wt %, 0.5 mL)/PS₂₈P2VP₂₈ star copolymer (0.1 mg/mL, 70 μ L) at pH 2 for different spreading solvents at surface pressure 0 mN/m): (a,b) toluene, (c) dichloromethane (CH₂Cl₂), and (d) tetrahydrofuran (THF). z-scale: 5 nm for (a–d) (topography) and 10° for (a,c,d); 30° for (b) (phase).

unfavorable due to stronger steric and electrostatic repulsions of interarms as compared to those of star copolymers with free P2VP ends, which are able to easily extend at the air–water interface and effectively reduce entropic repulsions.

Adsorption on the water surface rather than onto the solid graphene oxide surface seems to be more favorable because P2VP midblock can be, to some extent, extended into the water subphase (Scheme 1). We suggest that the preferential edge binding phenomena can be driven by the decrease in high surface energy of the graphene oxide edge via balancing the attraction force and reducing conformation entropy of star polymers. Notably, in the case of small molecules (e.g., oxygen and nitrogen gas), the graphene provides active edge sites for strong binding due to partial charges at the edges.⁴⁶ On the other hand, a preferential binding of small peptides to graphene can be induced by noncovalent bonding, that is, electrostatic or π – π interactions in solution. For instance, negatively charged amino acids on peptides are attracted to the edge of graphene sheets, while aromatic amino acid containing peptides were found to bind on the basal plane.⁴⁷

Effect of Spreading Solvent Polarity. The coverage of star copolymer on the surface of graphene oxide might be also related to solvent characteristics. It has been demonstrated that amphiphilic graphene oxide can stabilize the oil–water interface (e.g., aromatic and nonaromatic solvents) due to the graphitic domain.²³ In particular, a nonaromatic volatile organic solvent such as chloroform spreads on the graphene oxide and enables suspension on the water surface even after evaporation. Thus, further investigation of the influence of spread organic solvent on interface assembly was conducted by employing different organic polar solvents such as toluene, dichloromethane (CH₂Cl₂), and tetrahydrofuran (THF) for spreading star copolymer micelles in comparison with a good solvent, chloroform (CHCl₃) (Figure 6). Chloroform can play an important role in assembly because it is a good solvent for both PS and P2VP blocks and thus star macromolecules possess random coil–coil conformation without micelle formation in solution. Upon spreading at the air–water interface, it can facilitate the vertical phase segregation of star copolymers with collapsed hydrophobic PS core and ionized hydrophilic P2VP corona. This is beneficial for the hydrophilic aromatic pyridine

group on star copolymer to interact with hydrated graphene oxide sheets through ionic interaction.^{48,49}

In contrast to a nonselective polar organic solvent, the aromatic polar ones such as toluene are bad solvents for P2VP, and because P2VP arms are much longer than PS arms, we expect multimolecular micelle formation as was observed in Figure 6a and b. In the case of toluene, the star copolymer surface micelles dewetted due to contact of hydrophobic PS outer layer with the polar graphene oxide surface. It was shown that that toluene can be mixed with graphene oxide aqueous solution, producing graphene oxide-stabilized toluene/water emulsion and multimolecular micelles.²²

In the case of dichloromethane, large aggregates were observed with a morphology similar to those with chloroform (Figure 6c). However, the lower boiling temperature of dichloromethane (39.6 °C) (61.2 °C for chloroform) seems to limit single molecular level dispersion upon deposition. Finally, tetrahydrofuran (THF) endowed sparse star copolymer micelles both on graphene oxide and on the water surface (Figure 6d). One of the possible reasons is because the significant dipole moment of THF (1.75 D, as high as water 1.82 D) can enable the formation of stable dispersions of graphene oxides and adversely affect their interfacial stability. Such water-miscible THF seems to be insufficient to sustain star copolymer micelles at the interface with star copolymer micelles sinking into the water subphase during deposition.

CONCLUSIONS

In summary, we have observed the formation of peculiar biphasic morphology of star copolymers combined with graphene oxide sheets in Langmuir monolayers. Adsorption, spreading, and ordering of star polymer surface micelles on the basal plane and edge of in-plane amphiphilic monolayer graphene oxide were examined using a Langmuir trough. It was demonstrated that surface activity of solvated graphene oxide sheets makes it possible for star polymer surfactants to adsorb on the presuspended graphene oxide surface. As a result, this interface-mediated assembly led to micelle-decorated graphene oxide bilayer complexes with uniform spacing and organized morphology. Well-organized discrete micelle assem-

bly on the basal plane and edge of graphene oxide sheets is evidence for the presence of a strong affinity between star polymers and graphene oxide: electrostatic, hydrogen bonding, and π - π interactions between partially protonated heterocyclic pyridine units and negatively charged polar graphene oxide surface. The conformational transition (from pancake to brush) to minimize the entropic repulsion of highly branched charged arms in the vicinity of the sheets' edges was found to depend upon controlling parameters such as concentration and solvent polarity. Unlike the star polymer micelles on the water surface, the micelles on the basal plane of graphene oxide sheets remained incompressible under lateral compression due to the strongly repulsive confined arm status on their polar surface of graphene oxide. The densely packed, stable biphasic tile-like morphology of graphene oxide-star polymer complex films suggests the interfacially stable and mechanically stiff feature of graphene oxide sheets.

Interestingly, the surface coverage of star polymer unimicelles on the graphene oxide sheets was not affected by external assembly conditions after evaporative deposition in contrast to pressure-sensitive air-water interface. In contrast to the water surface where this repulsion can be reduced by submerging of P2VP arms into the water phase through a pH- and pressure-induced vertical conformational transition, this effect seems to be hindered by tethering to the graphene oxide surface. The obvious limited crossing of star unimicelles at the air-water surface over the graphene oxide surface under increased lateral surface pressure seems to be likely due to an energetically unfavorable reduction in conformational entropy of highly branched arms in the case that such a transition would occur from fluid water surface onto the confined solid graphene surfaces, as well as suggests the geometric and dimensional mismatch in two different types of surfactants. Vertically segregated polymer arm chain conformation across the air-water interface prevents the star polymers from sliding over the functionalized edge onto the surface of amphiphilic graphene oxide sheets. Also, the ability of graphene oxide to sustain high lateral surface pressure without sinking or folding can be attributed to the intrinsic stiffness as well as conformational surface tension upwardly applied on the continuous single sheets. The surface-assisted assembly strategy can facilitate large-scale film fabrication with biphasic "tile-like" morphology. This non-covalent surface assembly can offer a facile approach to fabrication of graphene oxide-inclusive ultrathin hybrid films for potential applications in heterogeneous catalysis and as highly sensitive sensing materials.

■ ASSOCIATED CONTENT

Supporting Information

Table S1 and Figures S1–S7. This material is available free of charge via the Internet at <http://pubs.acs.org>.

■ AUTHOR INFORMATION

Corresponding Author

*E-mail: vladimir@mse.gatech.edu.

Notes

The authors declare no competing financial interest.

■ ACKNOWLEDGMENTS

This work is supported by NSF-DMR 1002810 grant. We thank R. Kodiyath and Z. A. Comfor technical assistance.

■ REFERENCES

- (1) Hummers, W. S.; Offeman, R. E. Preparation of Graphitic Oxide. *J. Am. Chem. Soc.* **1958**, *80*, 1339–1339.
- (2) Kim, J.; Cote, L. J.; Huang, J. Two Dimensional Soft Material: New Faces of Graphene Oxide. *Acc. Chem. Res.* **2012**, *45*, 1356–1364.
- (3) Dreyer, D. R.; Park, S.; Bielawski, C. W.; Ruoff, R. S. The Chemistry of Graphene Oxide. *Chem. Soc. Rev.* **2010**, *39*, 228–240.
- (4) Liu, J.; Fu, S.; Yuan, B.; Li, Y.; Deng, Z. Toward a Universal "Adhesive Nanosheet" for the Assembly of Multiple Nanoparticles Based on a Protein-Induced Reduction/Decoration of Graphene Oxide. *J. Am. Chem. Soc.* **2010**, *132*, 7279–7281.
- (5) Mao, S.; Lu, G.; Yu, K.; Bo, Z.; Chen, J. Specific Protein Detection Using Thermally Reduced Graphene Oxide Sheet Decorated with Gold Nanoparticle-Antibody Conjugates. *Adv. Mater.* **2010**, *22*, 3521–3526.
- (6) Wang, Y.; Li, Z.; Hu, D.; Lin, C.-T.; Li, J.; Lin, Y. Aptamer/Graphene Oxide Nanocomplex for in Situ Molecular Probing in Living Cells. *J. Am. Chem. Soc.* **2010**, *132*, 9274–9276.
- (7) Wang, Z.; Huang, P.; Bhirde, A.; Jin, A.; Ma, Y.; Niu, G.; Neamati, N.; Chen, X. A Nanoscale Graphene Oxide–Peptide Biosensor for Real-Time Specific Biomarker Detection on the Cell Surface. *Chem. Commun.* **2012**, *48*, 9768–9770.
- (8) Chou, S. S.; De, M.; Luo, J.; Rotello, V. M.; Huang, J.; Dravid, V. P. Nanoscale Graphene Oxide (nGO) as Artificial Receptors: Implications for Biomolecular Interactions and Sensing. *J. Am. Chem. Soc.* **2012**, *134*, 16725–16733.
- (9) Liu, Z.; Robinson, J. T.; Sun, X.; Dai, H. PEGylated Nano-Graphene Oxide for Delivery of Water Insoluble Cancer Drugs. *J. Am. Chem. Soc.* **2008**, *130*, 10876–10877.
- (10) Kim, B. H.; Kim, J. Y.; Jeong, S.-J.; Hwang, J. O.; Lee, D. H.; Shin, D. O.; Choi, S.-Y.; Kim, S. O. Surface Energy Modification by Spin-Cast, Large-Area Graphene Film for Block Copolymer Lithography. *ACS Nano* **2010**, *4*, 5464–5470.
- (11) Lerf, A.; He, H.; Rorster, M.; Kilnowski, J. Structure of Graphite Oxide Revisited. *J. Phys. Chem. B* **1998**, *102*, 4477–4482.
- (12) Erickson, K.; Erni, R.; Lee, Z.; Alem, N.; Gannett, W.; Zettl, A. Determination of the Local Chemical Structure of Graphene Oxide and Reduced Graphene Oxide. *Adv. Mater.* **2010**, *40*, 4467–4472.
- (13) Dimiev, A.; Kosynkin, D. V.; Alemany, L. B.; Chaguine, P.; Tour, J. M. Pristine Graphite Oxide. *J. Am. Chem. Soc.* **2012**, *134*, 2815–2822.
- (14) Wang, X.; Bai, H.; Shi, G. Size Fractionation of Graphene Oxide Sheets by pH-Assisted Selective Sedimentation. *J. Am. Chem. Soc.* **2011**, *133*, 6338–6342.
- (15) Gudarzi, M. M.; Sharif, F. Self Assembly of Graphene Oxide at the Liquid–Liquid Interface: A New Route to the Fabrication of Graphene Based Composites. *Soft Matter* **2011**, *7*, 3432–3440.
- (16) Zou, J.; Kim, F. Self-Assembly of Two-Dimensional Nanosheets Induced by Interfacial Polyionic Complexation. *ACS Nano* **2012**, *6*, 10606–10613.
- (17) Cote, L. J.; Kim, F.; Huang, J. Langmuir-Blodgett Assembly of Graphite Oxide Single Layers. *J. Am. Chem. Soc.* **2009**, *131*, 1043–1049.
- (18) Gao, Y.; Chen, X.; Xu, H.; Zou, Y.; Gu, R.; Xu, M.; Jen, A. K.-Y.; Chen, H. Highly-Efficient Fabrication of Nanoscrolls from Functionalized Graphene Oxide by Langmuir–Blodgett Method. *Carbon* **2010**, *48*, 4475–4482.
- (19) Cheng, C.; Li, D. Solvated Graphenes: An Emerging Class of Functional Soft Materials. *Adv. Mater.* **2012**, *25*, 13–30.
- (20) Kulkarni, D. D.; Choi, I.; Singamaneni, S. S.; Tsukruk, V. V. Graphene Oxide–Polyelectrolyte Nanomembranes. *ACS Nano* **2010**, *4*, 4667–4676.
- (21) Hu, K.; Gupta, M. K.; Kulkarni, D. D.; Tsukruk, V. V. Ultra-Robust Graphene Oxide–Silk Fibroin Nanocomposite Membranes. *Adv. Mater.* **2013**, *25*, 2301–2307.
- (22) Kim, J.; Cote, L. J.; Kim, F.; Yuan, W.; Shull, K. R.; Huang, J. Graphene Oxide Sheets at Interfaces. *J. Am. Chem. Soc.* **2010**, *132*, 8180–8186.

- (23) Kim, F.; Cote, L.; Huang, J. Graphene Oxide: Surface Activity and Two-Dimensional Assembly. *Adv. Mater.* **2010**, *22*, 1954–1958.
- (24) Peleshanko, S.; Tsukruk, V. V. Assembling Hyperbranched Polymers. *J. Polym. Sci., Part B: Polym. Phys.* **2012**, *50*, 83–100.
- (25) Iatridi, Z.; Tsitsilianis, C. pH Responsive MWCNT–Star Terpolymer Nanohybrids. *Soft Matter* **2013**, *9*, 184–193.
- (26) Gröschel, A. H.; Löbbling, T.; Petrov, P. D.; Müllner, M.; Kuttner, C.; Wieberger, F.; Müller, A. H. E. Janus Micelles as Effective Supracolloidal Dispersants for Carbon Nanotubes. *Angew. Chem., Int. Ed.* **2013**, *52*, 3602–3606.
- (27) Tsitsilianis, C.; Chaumont, P.; Rempp, P. Synthesis and Characterization of Hetero-arm Star Copolymers. *Makromol. Chem.* **1990**, *191*, 2319–2328.
- (28) Tsitsilianis, C.; Voulgaris, D. Poly(2-vinylpyridine)-based Star-shaped Polymers. Synthesis of Heteroarm Star (A_nB_m) and Star-block (AB) $_n$ Copolymers. *Macromol. Chem. Phys.* **1997**, *198*, 997–1007.
- (29) Tsukruk, V. V.; Rinderspacher, F.; Bliznyuk, V. N. Adhesive and Friction Forces between Chemically Modified Silicon and Silicon Nitride Surfaces. *Langmuir* **1998**, *14*, 446–455.
- (30) Kodyath, R.; Choi, I.; Patterson, B.; Tsitsilianis, C.; Tsukruk, V. V. Interfacial Behavior of pH Responsive Ampholytic Heteroarm Star Block Terpolymers. *Polymer* **2012**, *54*, 1150–1159.
- (31) McConney, M. E.; Singamaneni, S.; Tsukruk, V. V. Probing Soft Matter with the Atomic Force Microscopies: Imaging and Force Spectroscopy. *Polym. Rev.* **2010**, *50*, 235–286.
- (32) Young, S. L.; Gupta, M.; Hanske, C.; Fery, A.; Sheibel, T.; Tsukruk, V. V. Utilizing Conformational Changes for Patterning Thin Films of Recombinant Silk Proteins. *Biomacromolecules* **2012**, *13*, 3189–3199.
- (33) Štěpánek, M.; Matějček, P.; Humpolíčková, J.; Havránková, J.; Podhájecká, K.; Špírková, K.; Tuzar, J.; Tsitsilianis, C.; Procházka, K. New Insights on the Solution Behavior and Self-assembly of Polystyrene/poly(2-vinylpyridine) ‘Hairy’ Heteroarm Star Copolymers with Highly Asymmetric Arms in Polar Organic and Aqueous Media. *Polymer* **2005**, *46*, 10493–10505.
- (34) Peleshanko, S.; Jeong, J.; Gunawidjaja, R.; Tsukruk, V. V. Amphiphilic Heteroarm PEO-*b*-PS $_m$ Star Polymers at the Air–Water Interface: Aggregation and Surface Morphology. *Macromolecules* **2004**, *37*, 6511–6522.
- (35) Gunawidjaja, R.; Peleshanko, S.; Tsukruk, V. V. Functionalized (X-PEO) $_2$ -(PS-Y) $_2$ Star Block Copolymers at the Interfaces: Role of Terminal Groups in Surface Behavior and Morphology. *Macromolecules* **2005**, *38*, 8765–8774.
- (36) Gunawidjaja, R.; Peleshanko, S.; Kirsten, L. G.; Tsitsilianis, C.; Tsukruk, V. V. Surface Morphologies of Langmuir–Blodgett Monolayers of PEOnPSn Multiarm Star Copolymers. *Langmuir* **2006**, *22*, 6168–6176.
- (37) Pispas, S.; Hadjichristidis, N.; Potemkin, I.; Khokhlov, A. Effect of Architecture on the Micellization Properties of Block Copolymers: A $_2$ B Miktoarm Stars vs AB Diblocks. *Macromolecules* **2000**, *33*, 1741–1746.
- (38) Choi, I.; Gunawidjaja, R.; Suntivich, R.; Tsitsilianis, C.; Tsukruk, V. V. Surface Behavior of PS $_n$ (P2VP-*b*-PtBA) $_n$ Heteroarm Stars. *Macromolecules* **2010**, *43*, 6818–6828.
- (39) Cote, L. J.; Kim, F.; Zhang, Z.; Huang, J. Tunable Graphene Oxide Surfactant Sheet: Wrinkles, Overlaps and Impact on Thin Film Properties. *Soft Matter* **2010**, *6*, 6096–6101.
- (40) Sheiko, S.; Zhou, J.; Arnold, J.; Neugebauer, D.; Matyjaszewski, K.; Tsitsilianis, C.; Tsukruk, V. V.; Carrillo, J.-M. Y.; Dobrynin, A. V.; Rubinstein, M. Perfect Mixing of Immiscible Macromolecules at Fluid Interface. *Nat. Mater.* **2013**, *1–6*, DOI: 10.1038/NMAT3651.
- (41) Kiriya, A.; Gorodyska, G.; Minko, S.; Stamm, M.; Tsitsilianis, C. Single Molecules and Associates of Heteroarm Star Copolymer Visualized by Atomic Force Microscopy. *Macromolecules* **2003**, *36*, 8704–8711.
- (42) Cox, J. K.; Yu, K.; Constantine, B.; Eisenberg, A.; Lennox, R. B. Polystyrene–Poly(ethylene oxide) Diblock Copolymers Form Well-Defined Surface Aggregates at the Air/Water Interface. *Langmuir* **1999**, *15*, 7717–7718.
- (43) Zhu, J.; Lennox, R. B.; Eisenberg, A. Interfacial Behavior of Block Polyelectrolytes. 2. Aggregation Numbers of Surface Micelles. *Langmuir* **1991**, *7*, 1579–1584.
- (44) Zhu, J.; Eisenberg, A.; Lennox, R. B. Interfacial Behavior of Block Polyelectrolytes. 1. Evidence for Novel Surface Micelle Formation. *J. Am. Chem. Soc.* **1991**, *113*, 5583–5588.
- (45) Zhu, J.; Eisenberg, A.; Lennox, R. B. Interfacial Behavior of Block Polyelectrolytes. 5. Effect of Varying Block Lengths on the Properties of Surface Micelles. *Macromolecules* **1992**, *25*, 6547–6555.
- (46) Radovic, L. Active Sites in Graphene and the Mechanism of CO $_2$ Formation in Carbon Oxidation. *J. Am. Chem. Soc.* **2009**, *131*, 17166–17175.
- (47) Kim, S. N.; Kuang, Z.; Slocik, J. M.; Jones, S. E.; Cui, Y.; Farmer, B. L.; MacAlpine, M. C.; Naik, R. R. Preferential Binding of Peptides to Graphene Edges and Planes. *J. Am. Chem. Soc.* **2011**, *133*, 14480–14483.
- (48) Gorodyska, G.; Kiriya, A.; Minko, S.; Tsitsilianis, C.; Stamm, M. Reformation and Metallization of Unimolecular Micelles in Controlled Environment. *Nano Lett.* **2003**, *3*, 365–368.
- (49) Lupitsky, R.; Roiter, Y.; Tsitsilianis, C.; Minko, S. From Smart Polymer Molecules to Responsive Nanostructured Surfaces. *Langmuir* **2005**, *21*, 8591–8593.